EXPERIMENTAL EVALUATION OF BRIDGE MONOLITHIC JOINTS UNDER SIMULATED SEISMIC LOADING

D. Timosidis[1] and S.J. Pantazopoulou[2]

[1] *Graduate Research Engineer, Dept. of Civil Engineering , Demokritus University of Thrace, Xanthi, Greece*
[2] *Professor, Laboratory of Reinforced Concrete, Dept. of Civil Engineering, Demokritus University of Thrace, Xanthi, Greece.*
Email:dtimosid@civil.duth.gr, pantaz@civil.duth.gr

ABSTRACT :

To evaluate the adequacy of the EN1998-2 design procedures for bridge monolithic connections between single pier column and superstructure, an experimental program on bridge joints under seismic loading was carried out. A total of six specimens were constructed, four of them representing connections in the direction transverse to the bridge axis and the remaining two representing connections along the bridge axis, at a scale of 18%. Specimens were tested under simulated seismic loading and combined gravity loads. Experimental recorded data of displacements, applied forces, strains, digital surface mapping and propagation of crack formation are used to characterize the strength and deformation capacity of the specimens. The results show that openings traditionally used as a passage for inspection of the box-shaped girders framing into the joints can compromise the connection performance and should be avoided. Column reinforcement comprising smaller diameter reinforcing bars anchored with a hook led to improved connection performance. Placement of the required joint reinforcement in the adjacent beams didn't affect the capacity of the joint whereas it helped avoiding the congestion problem caused by placing the required amount of vertical hoops inside the joint body.

KEYWORDS: bridge joints, shear strength, experiments, specimens, seismic loading

1. INTRODUCTION

The design of bridge monolithic connections received attention after the 1989 Loma Prietta earthquake, where bridge infrastructure suffered serious damage. Many of the reported damages and bridge collapses occurred because of inadequate detailing of the monolithic connections (joints) between pier and superstructure. Large scale experimental programs on bridge joints under simulated earthquake loading followed. Thewalt and Stojadinovic (1995) examined seven outrigger knee-joints modeling upper level connections of the same old-designed double deck bridge, scaled to 50% of prototype dimensions, evaluating various strengthening techniques. Sexsmith et al (1997) tested five two-column bridge support frames, at 45% scale, modeling an old-design typical bent of Vancouver's Oak Street bridge. Priestley et al (1997) examined experimentally one T-joint, at 75% scale, modeling a connection in an actual four-column bridge bent that had failed during the 1989 Loma Prietta earthquake. Ingham et al (1998) tested four outrigger joints representative of the design philosophy in 1991, at 33% scale. Lowes and Moehle (1999) examined three interior T-joints of three-column bridge bents, designed between 1950 and 1970, scaled to 33% of prototype dimensions. Mazzoni and Moehle (2001) tested two lower level joints of a double deck bridge that had failed at the 1989 Loma Prietta earthquake. The two specimens represented connections in both main bridge directions, designed according with Caltrans (1991), at 33% scale. Sritharan et al (2001) examined two three-column bents at 50% scale that were constructed according with the design practice after 1990. The effects of the cap beam prestressing were evaluated referring to the exterior and interior T-joint assessment. Naito et al (2001) tested six T-joints at 37.5% scale, representing bridge connections designed according with Caltrans (1995) with varying column geometry, reinforcement details and input joint shear stress. Pantelides et al (2001) tested in-situ three full-scale three-column bents constructed in 1963. Gibson et al (2002) examined four T-joints, at 50% scale, evaluating the

effects of the impulsive loading of near-field earthquakes in the behavior of old or recently designed joints.

The primary outcomes of this research passed into the design code development of Caltrans (2004) and EN1998-2 (2005). The above mentioned codes are the only codes in existence for bridge joint design under seismic loading. Caltrans (2004) compares the maximum total tensile stress developed in the middle of the joint panel with an empirical value obtained by the experimental experience. If the maximum tensile stress exceeds this value, the required joint reinforcement is calculated using a strut-and-tie analog proposed by Priestley et al (1996). Otherwise, minimum joint reinforcement is placed in the joint body. EN1998-2 (2005) calculates the maximum shear stress developing in concrete at the joint center using force equilibrium in both main joint directions. Concrete contribution and reinforcement contribution are separately taken into account in force equilibrium. If the maximum shear stress exceeds the concrete cracking shear stress, the required joint reinforcement is calculated by force equilibrium. Otherwise, minimum joint reinforcement is placed in the joint body. Both codes allow placement of a part of the vertical joint reinforcement in the beam at the sides of joint. Although a primary outcome of the experimental research was that anchorage conditions of pier longitudinal reinforcement within the joint is a critical parameter in the assessment of existing joints, Caltrans (2004) still allows the configuration of straight column anchorages inside joint areas, whereas EN1998-2 (2005) requires formation of hooks at the bar ends near the free joint face.

Despite the progress in recent design procedures, some issues related to bridge joint design under earthquake loading are still outstanding. Bond conditions of the main pier reinforcement anchorages are not explicitly taken into account, even if large diameter bars are used. The empirical requirement by EN1998-2 (2005) of formation of a hook at the end of anchorages is the only code rule towards this objective. The determination of the effective joint area is also an issue, especially for joints where framing members have hollow sections or are box girders. The discontinuity in the joint body owing to the design of openings for inspection passage is another issue that is common in bridge design practice but is not addressed by the recent codes. To examine these points an experimental program comprising six bridge joint specimens was carried out. Specimens were designed to represent joints between single pier column and superstructure, at 18% scale. All specimens were tested under simulated earthquake loading. In this paper, the experimental program is presented and the findings are used for evaluation of the EN1998-2 (2005) requirements.

2. EXPERIMENTAL PROGRAM ON BRIDGE JOINTS

All specimens (A1-A6) were designed to represent single column-to-superstructure connections, at a scale of 18%; four of them (A1-A4) in the direction perpendicular to the bridge axis (Fig.1a, Fig.1b) and the remaining two (A5 and A6) in the direction parallel to the bridge axis (Fig.1c). Specimens A1-A4 were designed to represent simultaneously two different types of joints: (a) between single column pier and single box superstructure with short pier (L_c<10m) and “strong” superstructure (J_M/M>10) where a significant moment is expected at the top of the pier under seismic excitation (Fig.1a) and (b) interior T-joints of a three-column bent supporting the superstructure through bearings (Fig.1b). A1 was designed and detailed according with EN 1998-2 (2005) (Fig.2a). A2 was designed with same geometry as A1, but with part of the required joint reinforcement in the beams at the sides of the joint, as alternatively proposed by EN 1998-2 (2005) to avoid reinforcement congestion problems (Fig.2b). A3 was designed with the same dimensions as A1 and A2, but with an opening for human passage at the joint body to check the practice of allowing inspection passages in monolithic bridge connections (Fig.2c). A4 was designed with a reduced cap beam width, to check if the increased width for cap beams required by EN 1998-2 (2005) is excessive (Fig.2d). A5 was designed also according with EN 1998-2 (2005), but in the direction along the bridge axis. This is the first reported test whereby the connection is between a solid pier and a box girder (Fig.2e). A6 was designed with the same dimensions as A5, but with an opening for human passage in the joint body to evaluate the influence of the openings in the other bridge axis (Fig.2f).

All reinforcement used for the construction of the specimens was typical Greek S500 deformed reinforcement, with nominal yield strength f_y=500MPa, maximum to yield strength ratio $1.15 \le f_u/f_y \le 1.35$, and a strain ductility at failure $\varepsilon_u/\varepsilon_y \ge 7.5$. Concrete material properties were determined from standard cylinder tests. Table 1

summarizes the concrete material test results.

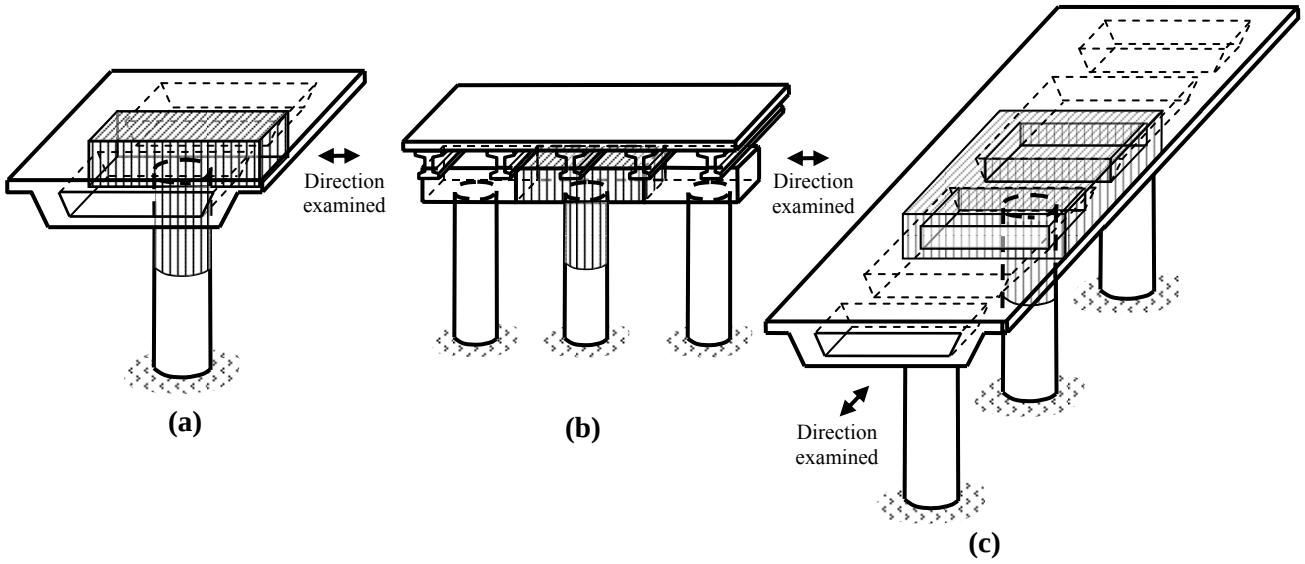

Figure 1 Type of joints: (a) between single column pier and single box superstructure in the direction perpendicular to bridge axis (A1 to A4 specimens), (b) between interior column and cap-beam of a three-column bent (specimens A1 to A4) and (c) between single column pier and single box superstructure in the direction along bridge axis (A5 and A6 specimens).

Specimens were placed in the testing frame at 90° from their actual position as shown in Figure 3. All specimens were initially subjected to the simulated gravity loads that were applied by stressing four high strength rods and two spreader beams placed at the top and the bottom of the columns. The reaction loads produced shears and moments in the beams at the joint faces equal to scaled values expected in the prototype structure and an axial force in the columns equal to $N_c=0.02A_g f_{cm}$. The column axial load was controlled mechanically during the tests, by loosening the rods when its value exceeded 1.5 times the initially applied value. Once the gravity load had been applied, earthquake lateral loads were simulated by applying a force in a quasi-static manner at the end of the column through an idealized pin. This force alternated back and forth transversally to the column longitudinal axis to simulate cyclic loading. Three cycles were performed for each loading step: (a) at $0.50F_y$, $0.75F_y$ and $1.00F_y$, where F_y is the estimated load for first yielding (column yielding) of the specimens by section analysis of the critical section, (b) at $1.50\delta_y$, $2.00\delta_y$, $4.00\delta_y$ and $6.00\delta_y$, where δ_y was the recorded lateral displacement of the column end at the first cycle of $1.00F_y$ loading step (Fig.4). Tests were terminated when exceeding the actuators' displacement amplitude (i.e., with displacement control after first yielding of the specimens).

Recorded experimental measurements included forces, displacements, strains and pullout slip. Column axial force and lateral applied force were recorded by calibrated load cells. Concrete surface strains were obtained through non-contact digital-imaging of a network of targets adhered on the specimens' surface.

3. BEHAVIOR OF TEST SPECIMENS

Specimen performance was gauged from experimental records of: lateral displacement at the column end versus applied lateral force, and joint distortion versus developed joint shear stress. Envelopes to these experimental response curves are plotted in Figures 5a and 5b, respectively. Lateral displacement values at the column end were corrected at each loading point by subtracting contributions owing to rotation of the testing frame. Joint shear stress was calculated at every loading point from free body diagram of the specimen and force equilibrium of the joint body. Joint distortion was calculated from the measurements of the two DTs at the diagonals of the joint face or the measurement of the same distances on the digital captures. The average strain developed at the extreme column main bars inside the plastic hinge length and the slip of the extreme column anchorages inside the joint were also calculated during the tests.

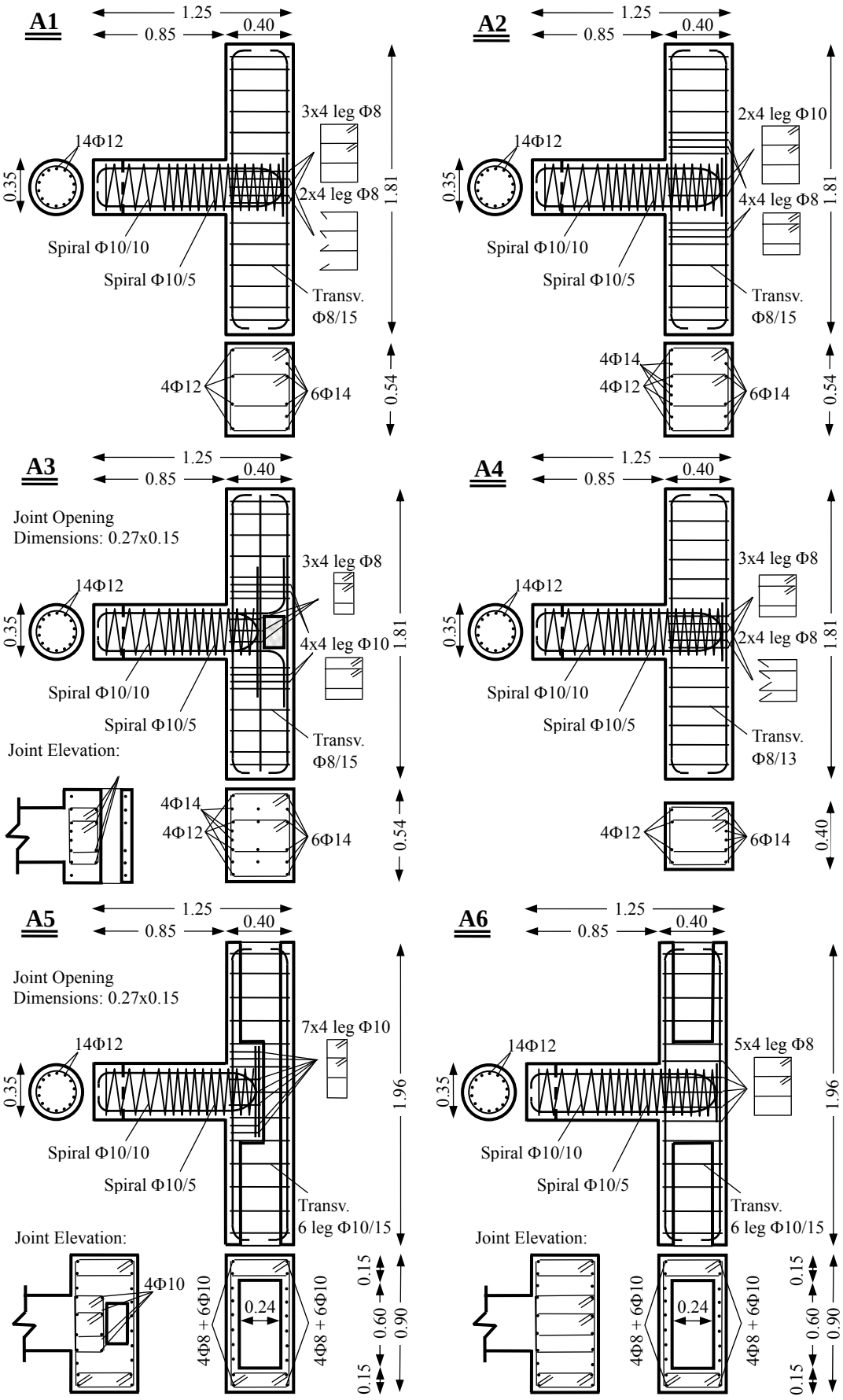

Figure 2 Geometry and reinforcement arrangement of Group A specimens

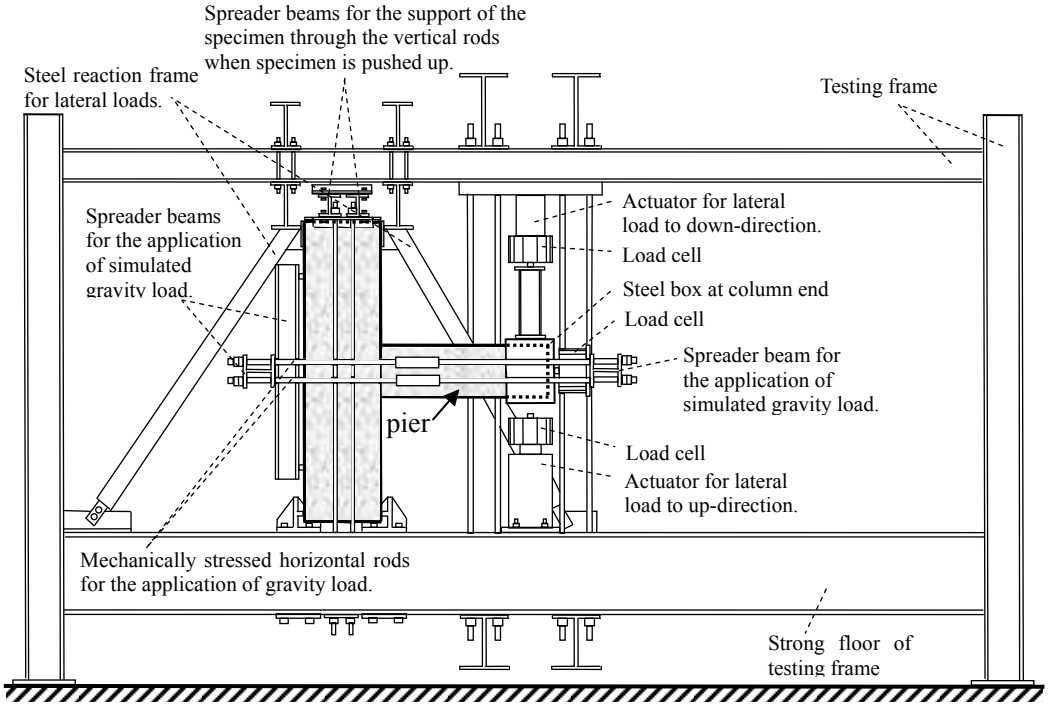

Figure 3 Test setup

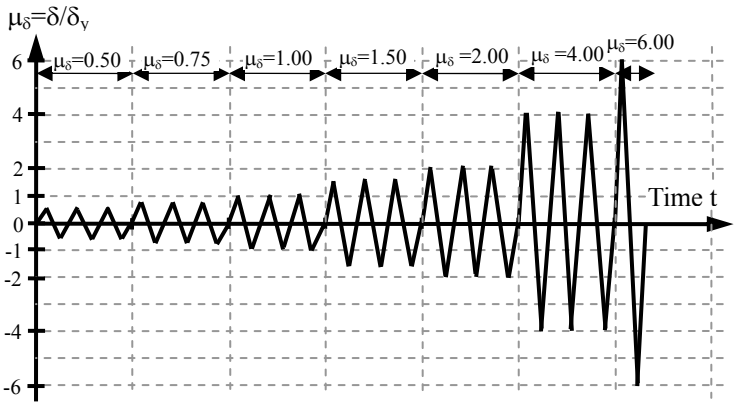

Figure 4 Imposed lateral displacement

Table 1 Concrete material properties for all specimens

Specimen	A1	A2	A4	A4	A5		A6	
					beam	column	beam	column
Days of test	176	251	259	302	30	28	88	86
f_{cm} (MPa)	27.55	29.14	29.30	29.85	26.00	33.95	26.30	45.00
$E_{cm,o}$ (MPa)	9910	12445	11725	10705	9440	15595	5970	14645

Specimens A1 and A2 behaved similarly during the test. During the force-control cycles both specimens showed only flexural cracks in the column critical area. At the next loading steps, of $1.50\delta_y$ and $2.00\delta_y$, the column flexural cracks propagated and became wider, while minor diagonal shear cracks also appeared on the column faces. The first diagonal cracks appeared on the joint faces also for $1.50\delta_y$. Joint diagonal cracks continued at the bottom beam face towards the perimeter of the column, in a radial direction. Joint yielding occurred for the first cycle at $1.50\delta_y$ for both specimens as was evidenced in the shear stress-distortion diagrams (Fig.5b); however its occurrence could not be deciphered from external observation only. Joint shear stress at first yielding of the joint was estimated at 2.00MPa and 1.60MPa, for A1 and A2, respectively. The joint shear strength for A1 was 2.6 MPa and was achieved during the first cycle of $2.00\delta_y$. For A2, the maximum attainable joint shear stress was

equal to 2.62MPa and was achieved at two points of the test, i.e. in the first cycle of $2.00\delta_y$ and in the first cycle of $4.00\delta_y$, confirming the excellent behavior of the specimen. After the second cycle at $2.00\delta_y$ the joint diagonal cracks extended lightly, whereas the flexural column cracks near joint-column interface became wide indicating slip of the anchorages of the main column reinforcement inside the joint. Spalling of concrete cover at the critical column area began and extended at the loading steps that followed. Tests were concluded when buckling of column longitudinal reinforcement begun. The slip of the extreme column longitudinal reinforcement at the end of the tests reached the value of 30.0mm, whereas at first yielding of the joints it did not exceed the value of 3.0mm. The overall behavior of the specimens was in conformity with the design philosophy used, with the damage concentrated at the column critical regions and the joints entering the plastic range after the first cycle of $1.50\delta_y$, but showing minor diagonal cracking until the end of the tests.

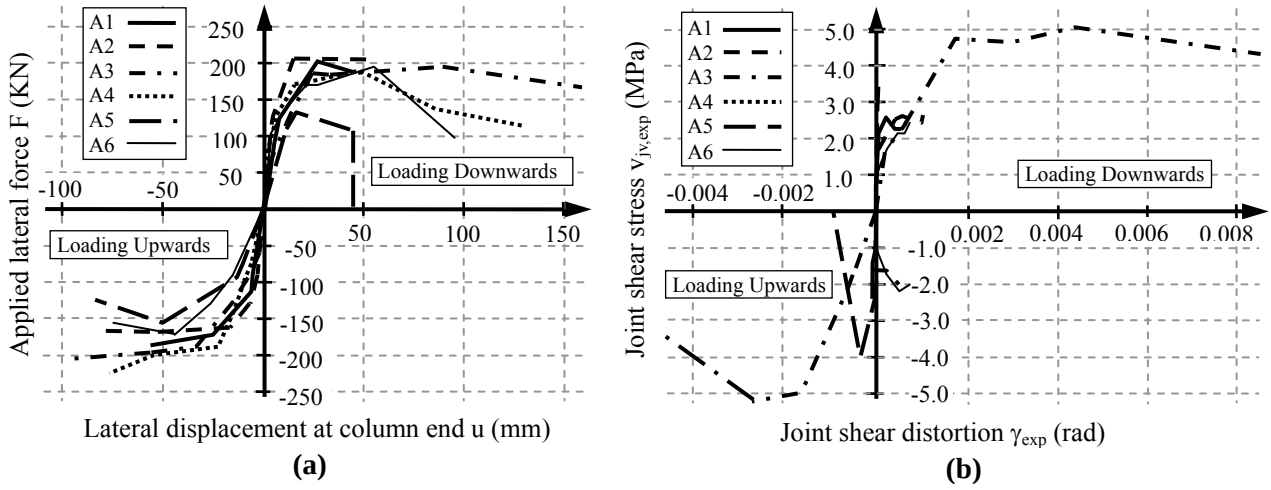

Figure 5 Response envelope: (a) lateral load vs. displacement (b) joint shear stress vs joint distortion

Specimen A3 (with an opening in the joint body) showed column flexural cracks from the first cycles of loading that continued to propagate from cycle to cycle. Minor diagonal shear cracks formed at the column faces, increasing in width until the first cycle at $4.00\delta_y$. The first shear cracks in the joint appeared at $0.75F_y$. The ends of the joint diagonal cracks turned parallel to the longitudinal column reinforcement for $1.00F_y$, indicating large values of anchorage slip. At loading steps of $1.50\delta_y$, $2.00\delta_y$ and $4.00\delta_y$ shear cracks in the joint became about 1.0mm, 1.2mm and 2.5mm wide, respectively. At $2.00\delta_y$ minor flexural cracks were formed at the top beam face parallel to the edges of the opening, whereas concrete spalling at both the joint faces and the column critical region began at $4.00\delta_y$. At $6.00\delta_y$ the joint shear cracks didn't propagate any further, but the column longitudinal reinforcement buckled, leading to loss of the specimen's capacity. The developed joint shear stress was estimated at 3.40MPa at the point of first joint yielding, but reached the maximum value of 5.25MPa for $4.00\delta_y$. The associated distortion was estimated equal to 0.0011rad and 0.0044rad, respectively (these values concern the solid part of the joint underneath the opening.) Despite the opening in the joint body, the specimen sustained satisfactorily the same loading history as A1 and A2 (Fig.5a), showing column flexural failure. Note that the joint developed maximum shear strains that exceeded 0.009rad and 0.005rad for loading downwards and upwards, respectively (Fig.5b). As a matter of fact, the joint developed shear strains about 10 times as high as in A1 and A2, without loss of capacity, although degradation was evident in the last loading cycle. The good joint response is attributed to the favorable anchorage conditions of column longitudinal reinforcement with an end hook; this point is confirmed by the estimated anchorage slip of the extreme column reinforcement which did not exceed the corresponding value of specimen A2 (30.0mm.)

Specimen A4 showed almost the same behavior as A1 and A2 during the test procedure. In contrast with specimens A1 and A2, the first shear minor cracks appeared at the joint faces at $0.75F_y$ and continued to propagate for every loading step, forming a dense net of diagonal cracks until the end of the test. Although the cap beam and as a result the joint of A4 was designed with reduced width, the joint sustained successfully the loading envelope. The joint shear stress at first yielding of the joint (at $1.00F_y$) was equal to 2.28MPa and attained a maximum of 3.88MPa for peak load. The specimen showed flexural column failure, with spalling of

cover concrete at the column critical region in the second cycle of $4.00\delta_y$ and buckling of longitudinal column reinforcement at $6.00\delta_y$. The test was concluded upon termination of the range of the actuator, although the specimen could resist till the end of the test a high percentage of the maximum induced loading. Slip of the extreme longitudinal column reinforcement at first joint yielding was estimated about 1.0mm.

For specimen A5, the first flexural cracks in the column critical region and the first shear minor cracks in the joint faces were observed already in the first cycle at $0.50F_y$ and propagated during the following cycles. For $0.75F_y$ the diagonal shear cracks at the joint faces propagated along the anchorages of the longitudinal column reinforcement, indicating large values of anchorage slip. In the first cycle at $1.00F_y$, diagonal cracks in the joint became 2-3mm wide and spalling of the concrete cover of the joint reinforcement began, while the column flexural cracks at joint-column interface increased suddenly. Upon reversal of the load, the specimen's displacement increased abruptly at an almost constant value of force. In the second cycle at $1.00F_y$ the specimen failed in shear (Fig.5a) because of punching of the cap beam along the joint boundaries. Shear punching was accompanied by concrete spalling at the bottom beam face along a circumferential line, about 10-20cm far from the perimeter of the connected column. At specimen failure, flexural cracks on the top beam face were also observed; the cracks were wider at the points of beam-joint interfaces. The maximum joint shear stress at failure (first cycle at $1.00F_y$) was recorded equal to 4.00MPa, whereas the associated joint distortion was 0.00037rad. In the second cycle at $1.00F_y$ the joint distortion exceeded the value of 0.001rad that was the highest value of distortion that was observed among all specimens during the loading step of $1.00F_y$. The value of anchorage slip of the longitudinal column reinforcement exceeded 20.0mm at the end of the test; this was also the highest value that was observed among all specimens for the loading step of $1.00F_y$.

Specimen A6 showed flexural cracks in the column critical area without any shear cracks at the joint faces during the force-control cycles of the test. At loading steps of $1.50\delta_y$ and $2.00\delta_y$, the flexural cracks at the column critical region propagated, while shear minor cracks appeared at the column faces. The first diagonal cracks also appeared on the joint faces. The joint shear cracks were extended to the bottom beam face until the perimeter of the column in a direction towards the center of the column section. At $4.00\delta_y$, spalling of concrete in the column critical section was observed, whereas the column flexural cracks near the joint-column interface propagated, indicating large values of anchorage slip of the column longitudinal reinforcement. For $6.00\delta_y$ the column longitudinal bars buckled and the specimen started to lose capacity (Fig.5a). Joint yielding occurred at $1.00\delta_y$ with the joint distortion exceeding the value of 0.0002rad and the joint shear stress reaching the value of 1.80MPa. Maximum attained joint shear stress was 2.48MPa in the first cycle at $4.00\delta_y$, while the associated distortion was 0.0007rad. Joint yielding was associated with slip of column longitudinal reinforcement equal to 1.7mm for $1.00\delta_y$, but reached the value of 20.0mm in the end of the test. Overall, the behavior of specimen A6 is judged satisfactory. The joint maintained its capacity, whereas the column showed flexural failure. The test ended because of termination of the loading range.

4. CONCLUSIONS

All specimens that modeled T-joints in the direction perpendicular to the bridge axis (A1 to A4) performed satisfactory under simulated earthquake loading, with flexural failure in the column critical area. Joints of A1, A2 and A4 showed excellent response, developing a net of minor shear cracks. The crack net was denser for A4 that was designed with a reduced cap beam width, however without affecting its overall behavior. The joint assessment of A3 was proved to be much better than expected. Although wide diagonal shear cracks and concrete spalling were observed on the joint faces of A3, the joint sustained the imposed reversed cyclic loading history and the specimen failed because of exceeding the column's flexural overstrength. The satisfactory behavior of A1 to A4 specimens (especially this of A3) is attributed to the good anchorage conditions of the Φ12 longitudinal column bars that were formed with a hook at the end of their anchorage.

Specimens that represented T-joints in the direction along the bridge axis (A5 and A6) showed a different behavior under reversed cyclic loading. Specimen A5 with the opening in the joint body failed in punching shear of the cap beam along the joint boundaries. The behavior of A6 was satisfactory with flexural failure in the

column critical area and wide hysteresis loops. Thus, construction of inspection openings in the joint bodies is judged destructive and should be avoided; in such cases the critical design direction is along the bridge axis.

As a result, the detailing of monolithic connections between pier and superstructure according with EN1998-2 (2005) leads to very good assessment of the connections under earthquake loading. Special care should be provided for the design of the anchorages of the pier longitudinal reinforcement according with EN1992-2 (2005) to prevent joints from anchorage pullout. The placement of a percentage of the required vertical joint reinforcement in the beams at the joint sides, as EN1998-2 (2005) alternatively proposes, doesn't reduce the joint strength, whereas it facilitates the placement of the reinforcement in practice. In any case, the creation of in-continuities in the joint body as are the openings for human passing should be avoided.

ACKNOWLEDGEMENTS

Funding for this work was provided by the Hellenic General Secretariat for Research and Technology through Research Program ASPROGE

REFERENCES

Caltrans (1991). Bridge Design Specifications, California Transportation Agency, California.
Caltrans (1995). Bridge Design Specifications, California Transportation Agency, California.
Caltrans (2004). Seismic Design Criteria Ver.3.1, California Transportation Agency, California.
European Committee for Standardization (2005). Eurocode 2: Design of Concrete Structures – Part 2: Concrete Bridges. Design and detailing rules, CEN, Brussels.
European Committee for Standardization (2005). Eurocode 8: Design of Structures for Earthquake Resistance – Part 2: Bridges, CEN, Brussels.
Gibson, N., Filiatrault, A. and Ashford, S.A. (2002). Performance of Beam to Column Bridge Joints Subjected to a Large Velocity Pulse. *PEERC Report* **2002:24**, 1-87.
Ingham, J.M., Priestley, M.J.N. and Seible, F. (1998). Cyclic Response of Bridge Knee Joints with Circular Columns. *ICP J. of Earthquake Eng.* **2:3**, 357-390.
Lowes, L.N. and Moehle, J.P. (1999). Evaluation of Retrofit of Beam-Column T-Joints in Older Reinforced Concrete Bridge Structures. *ACI Structural J.* **96:4**, 519-533.
Mazzoni, S. and Moehle, J.P. (2001). Seismic Response of Beam-Column Joints in Double Deck Reinforced Concrete Bridge Frames. *ACI Structural J.* **98:3**, 259-269.
Naito, C.J., Moehle, J.P. and Mosalam, K.M. (2001). Experimental & Computation Evaluation of Reinforced Concrete Bridge Beam-Column Connections for Seismic Performance. *PEERC Report* **2001:08**, 1-232.
Pantelides, C., Gergely, J. and Reaveley, L. (2001). In-Situ Verification of Rehabilitation & Repair of R/C Bridge Bents under Simulated Seismic Loads. *EERI Earthquake Spectra* **17:3**, 507-530.
Priestley, M.J.N., Seible, F. and Calvi, M. (1996). Seismic Design and Retrofit of Bridges, J.Wiley & Sons, New York, U.S.A.
Priestley, M.J.N., Seible, F., MacRae, G.A. and Chai, Y.H. (1997). Seismic Assessment of the Santa Monica Viaduct Bent. *ACI Structural J.* **94:5**, 513-524.
Sexsmith, R., Anderson, D. and English, D. (1997). Cyclic Behavior of Concrete Bridge Bents. *ACI Structural J.* **94:2**, 103-114.
Sritharan, S., Priestley, M.J.N. and Seible, F. (2001). Seismic Design and Experimental Verification of Concrete Multiple Column Bridge Bents. *ACI Structural J.* **98:3**, 335-346.
Thewalt, C.R. and Stojadinovic, B. (1995). Behavior of Bridge Outrigger Knee Joint Systems. *EERI Earthquake Spectra* **11:3**, 477-508.